An experimental Indian gravimetric geoid model using Curtin University's approach

R. Goyal[1,2,*], W.E. Featherstone[2,1], S.J. Claessens[2], O. Dikshit[1], N. Balasubramanian[1]

1) Department of Civil Engineering, Indian Institute of Technology Kanpur, Kanpur 208016, India; rupeshg@iitk.ac.in, onkar@iitk.ac.in, nagaraj@iitk.ac.in

2) School of Earth and Planetary Sciences, Curtin University of Technology, GPO Box U1987, Perth WA 6845, Australia; w.featherstone@curtin.edu.au, s.claessens@curtin.edu.au

ORCIDs: R Goyal ((0000-0002-2178-3265); W.E. Featherstone (0000-0001-9644-4535); S.J. Claessens (0000-0003-4935-6916); O. Dikshit (0000-0003-3213-8218)

This manuscript is submitted to "Terrestrial, Atmospheric and Oceanic Sciences"

Running title: Experimental Indian gravimetric geoid model

Three Key Points:

a) Indian gravimetric geoid and quasigeoid models are developed using the CUT method

b) The peculiarities of the Indian geodetic data are discussed

c) Intermediate results of geoid computation methodology are presented for the whole of India

Corresponding author: Ropesh Goyal, rupeshg@iitk.ac.in; ropeshgoyal2809@gmail.com

ABSTRACT

Over the past decade, numerous advantages of a gravimetric geoid model and its possible suitability for the Indian national vertical datum have been discussed and advocated by the Indian scientific community and national geodetic agencies. However, despite several regional efforts, a state-of-the-art gravimetric geoid model for the whole of India remains elusive due to a multitude of reasons. India encompasses one of the most diverse topographies on the planet, which includes the Gangetic plains, the Himalayas, the Thar desert, and a long peninsular coastline, among other topographic features. In the present study, we have developed the first national geoid and quasigeoid models for India using Curtin University's approach. Terrain corrections were found to reach an extreme of 187 mGal, Faye gravity anomalies 617 mGal, and the geoid-quasigeoid separation 4.002 m. We have computed both geoid and quasigeoid models to analyse their representativeness of the Indian normal-orthometric heights from the 119 GNSS-levelling points that are available to us. A geoid model for India has been computed with an overall standard deviation of ±0.396 m but varying from ±0.03 m to ±0.158 m in four test regions with GNSS-levelling data. The greatest challenge in developing a precise gravimetric geoid for the whole of India is data availability and its preparation. More densely surveyed precise gravity data and a larger number of GNSS/levelling data are required to further improve the models and their testing.

Keywords: Geoid, quasigeoid, India, Curtin University's approach

1. INTRODUCTION

Ideally, Stokes's (1849) integral should be implemented over the entire Earth with continuous gravity anomalies on the geoid and with the condition that there must not be any gravitating masses above it. However, in practice, the availability of gravity observations is limited to a specific area, so the integration domain has to be truncated. Also, the gravity anomalies usually exist discontinuously on or above the Earth's surface so various types of downward continuation and regularisation have been proposed. The gaps between theoretical and practical aspects induce several kinds of errors, which geodesists have tried to reduce, but usually requiring assumptions and approximations.

Based on various ideas, philosophies and numerical approaches, what we consider the four most commonly used approaches/techniques are adopted for geoid computation experiments in India. i) geoid/quasigeoid computation methodology developed at the University of Copenhagen, Denmark (Forsberg 1984, 1985; Forsberg and Tscherning 2008) implemented in the public-domain GRAVSOFT package, ii) the Stokes-Helmert method developed at the University of New Brunswick (UNB), Canada (Vaníček and Kleusberg 1987; Vaníček and Martinec 1994; Vaníček et al. 1999; UNB, 2002; Ellmann and Vaníček 2007), iii) the Least Squares Modification of Stokes formula with Additive Corrections (LSMSAC) method developed at the Royal Institute of Technology (KTH), Sweden (Sjöberg 1984, 1991, 2003; Ågren 2004), and iv) geoid/quasigeoid computation methodology developed at Curtin University of Technology (CUT), Australia (Featherstone 2000, 2003; Featherstone et al. 1998, 2001, 2011, 2018). There are of course other approaches, such as radial basis functions (e.g., Li 2018; Liu et al. 2020), but perhaps not yet applied as widely. The application areas of the above four approaches are listed in Goyal et al. (2021b).

For India, the first geoid map was developed more than five decades ago. It was based on astrogeodetic observations (Fischer 1961) and with respect to the Everest 1956 ellipsoid (cf. Singh and Srivastava 2018). No more information is available on this geoid, apart from distorted hardcopy contour maps that are difficult to digitise reliably. The levelled height information presently available

67 in India is more than a century old. When these heights were observed, neither the concept of foresight
68 and backsight levelling nor the use of invar staves were considered. Observed gravity values were
69 not available as this was before the development of the low-cost portable relative gravimeter. The
70 Indian vertical datum defined in 1909 was based on constraining the levelling to nine tide-gauges
71 along the Indian coast to zero height (Burrard 1910). We will show later that this approach may have
72 caused a north-south tilt (cf. Fischer 1975; 1977), most probably due to the ocean's time-mean
73 dynamic topography (cf. Featherstone and Filmer 2012).

74 Frequent seismic activity in various parts of the Indian sub-continent and so-caused crustal
75 movement also necessitate the introduction of a new height system, probably to be based on
76 geopotential numbers and Helmert's orthometric heights (or 'rigorous' orthometric heights as
77 formulated by Santos et al. 2006). The Survey of India (SoI) carried out a re-levelling program [2007-
78 2017] with gravity observations at fundamental benchmarks to provide a densified network of
79 Helmert's orthometric heights as a part of the Redefined Indian Vertical Datum 2009 (Singh 2018;
80 G&RB 2018). However, these data are not yet in the public domain, so we are unable to use them to
81 validate our geoid and quasigeoid models. In addition, the national geodetic agencies have proposed
82 to compute a precise national geoid model to serve as the new vertical datum for the country. This
83 can be viewed as following the suit of New Zealand (LINZ 2016), Canada (Véronneau and Huang
84 2016), and the USA (NGS 2017; 2019). Such an approach is being considered in many other countries
85 too.

86 Researchers and government organisations have made some efforts to develop local
87 gravimetric geoid models for regions in India (Singh 2007; Carrion et al. 2009; Srinivas et al. 2012;
88 Mishra and Ghosh 2016, Singh and Srivastava 2018), but only using the GRAVSOFT package with
89 residual terrain modelling (Forsberg 1985). Despite these efforts, a state-of-the-art national
90 gravimetric geoid model for the whole India remains elusive (Goyal et al. 2017). Therefore, in this
91 study, we present the first-ever nationwide geoid and quasigeoid computation results over India with

92 the available data sets using the CUT method implemented using our own computation package
93 developed in MATLAB ™.

94

95 2. DATASETS

96 2.1 Terrestrial Gravity

97 Pointwise observed gravity data is confidential in India. Therefore, with this predicament, we
98 obtained a grid of Indian terrestrial gravity data from GETECH (https://getech.com/) that is claimed
99 to come from the Gravity Map Series of India (GMSI), a joint project of five Indian organisations,
100 viz., SoI, Geological Survey of India (GSI), Oil and Natural Gas Corporation (ONGC), National
101 Geophysical Research Institute (NGRI) and Oil India Limited (cf. Tiwari et al. 2014). The GETECH
102 gravity data comprises a 0.02˚×0.02˚ grid of simple Bouguer gravity anomalies over India (except a
103 for few regions in northern India), with an overall estimated precision of ±1.5 mGal (GETECH,
104 2006). According to the GETECH manual for Indian gravity data, they used i) the normal gravity
105 formula from WGS84 (Macomber 1984)

106 $$\gamma_{0\_WGS84} = 978032.67714\left[\frac{1+0.00193185438639\sin^2\phi}{\sqrt{1-0.00669437999013\sin^2\phi}}\right] mGal \quad (1)$$

107 ii) a second-order free-air correction given by

108 $$\delta g_{FAC}^{GETECH} = \left(0.3083293357 + 0.0004397732\cos^2\phi\right)h - 7.2125\times10^{-8}h^2 \text{ mGal} \quad (2)$$

109 iii) the following atmospheric correction (Ecker and Mittermayer 1969)

110 $$\delta g_{atm}^{GETECH} = \begin{cases} 0.87e^{-0.116H^{1.047}}\, mGal, H > 0km \\ 0.87 mGal \qquad\quad , H <= 0km \end{cases} \quad (3)$$

111 and iv) the simple planar Bouguer correction

112 $$\delta g_{BC}^{GETECH} = -0.04191\rho H \; mGal \approx -0.1119H \; mGal \quad (4)$$

where γ_{0_WGS84} is normal gravity on the WGS84 level ellipsoid, δg_{FAC}^{GETECH} is the free-air correction, ϕ is the geodetic latitude, h is the ellipsoidal height (in m), H is the elevation (in km for Eqn. 3 and m for Eqn. 4), δg_{atm}^{GETECH} is the atmospheric correction, δg_{BC}^{GETECH} is the planar Bouguer correction and ρ is the constant topographical density of 2,670 kg/m3. We re-computed the free-air gravity anomalies (Δg) from the GETECH data so as to be more compatible with the CUT approach by using

$$\Delta g = \Delta g_{SBA}^{GETECH} + 0.1119H + \gamma_{0\_WGS84} - \delta g_{FAC}^{GETECH} - \delta g_{atm}^{GETECH} - \gamma_{0\_GRS80} + \delta g_{FAC}^{CUT} + \delta g_{atm}^{CUT} \quad (5)$$

where, Δg_{SBA}^{GETECH} are simple Bouguer anomalies from GETECH and

$$\delta g_{FAC}^{CUT} = \gamma_{0\_GRS80}\left(\frac{2}{a}\left(1+f+m-2f\sin^2\phi\right)H - \frac{3}{a^2}H^2\right) \quad (6)$$

$$\gamma_{0\_GRS80} = \gamma_a\left(\frac{1+k\sin^2\phi}{\sqrt{1-e^2\sin^2\phi}}\right) \quad (7)$$

$$\delta g_{atm}^{CUT} = 0.871 - 1.0298\times10^{-4}H + 5.3105\times10^{-9}H^2 - 2.1642\times10^{-13}H^3 + 9.5246\times10^{-18}H^4 - 2.2411\times10^{-22}H^5 \quad (8)$$

For GRS80, $a = 6378137m,\ e^2 = 0.0066943800229,\ m = 0.0034478600308,\ f = 1/298.257222101$ $\gamma_a = 978032.67715mGal,\ k = 0.001931851353$ (Moritz 2000). The descriptive statistics of the differences between the free-air anomalies from the GETECH data and re-computed free-air anomalies are (in mGal): min=-0.001, max=0.188, mean=0.002, STD=±0.007. It should be noted that we have used H instead of h (ellipsoidal heights) in Eqn. 2 because we believe that there might be a typographical error in the GETECH manual. The rationale being that with the use of h we would obtain gravity disturbances and not gravity anomalies (cf. Hackney and Featherstone 2003). A blanket accuracy estimate of the reconstructed free-air anomalies from the GETECH Bouguer anomalies is

±2.4 mGal, calculated using the DEM error in the CUT reconstruction technique as per $\sigma_{FA} = \sqrt{\left(1.5\times10^{-5}\right)^2 + \left(2\pi G\rho\times17.3\right)^2}$.

For the oceanic regions surrounding India, we used free-air gravity anomalies (Version 28.1) from the Scripps Institute of Oceanography (SCRIPPS, https://topex.ucsd.edu/marine_grav/mar_grav.html) which has an overall root mean square error of ±1.23 mGal (Sandwell et al. 2019). The SCRIPPS data is also accompanied with an error grid that we have shown, for our study area, in Figure 1. The data contains a 1'x1' grid that also covers the land, but we used the SCRIPPS data only for the oceanic region because the land data, in the SCRIPPS dataset, is from EGM2008 to avoid aliasing (Gibbs fringing) at the coasts.

PLACE FIGURE 1 NEAR HERE

We do not have gravity data from the countries neighbouring India and a well distributed sufficient data coverage is not available in the Bureau Gravimetrique International (https://bgi.obs-mip.fr/) archives either (Country: no. of gravity data points - Pakistan: 1270, Bangladesh: 25, Sri Lanka: 48, Myanmar: 71, Afghanistan: 1649, China: 446, Nepal: 617 and Bhutan: 0.). Therefore, we constructed a 0.02˚×0.02˚ grid of free air anomalies over land using EGM2008 (Pavlis et al. 2012; 2013) up to degree and order (d/o) 900 to fill-in the land gravity anomaly data in and around India where the GETECH data is not available, including Nepal, China, Pakistan, Sri Lanka, Bangladesh, Bhutan, Afghanistan and Myanmar. The specific d/o 900 was chosen because EGM2008 uses proprietary data up to d/o 900 (Pavlis et al. 2013).

As discussed next, we merged these three datasets to get a complete free-air gravity anomaly grid of 0.02°x0.02°, avoiding aliasing or the contamination of land data (both GETECH and EGM2008 individually) with the marine data or vice-versa.

There exist numerous sophisticated space-domain and frequency-domain methods for merging heterogenous gravity anomaly datasets (e.g., Strykowski and Forsberg 1998; Olesen et al. 2002; Catalao 2006; McCubbine et al. 2017). However, we chose to work with the comparatively

157 straightforward CUT space-domain method (cf. Featherstone et al. 2011; 2018). This choice is
158 somewhat arbitrary because we are working with the land gravity of unknown quality, and the
159 strategy that we use has already been implemented in the computation of the Australian quasigeoid,
160 which is an island nation and approximately 2.3 times larger than India. Other methods can also be
161 tested, but it is left for the time when sufficient marine and airborne gravity data along with reliable
162 terrestrial gravity data will be available over India.

163 In the adopted method, the GETECH-derived free-air anomaly grid is superimposed over the
164 EGM2008 (d/o 900) derived gravity anomalies. The gravity anomalies of the latter dataset at the
165 overlapping grid nodes are replaced by the gravity anomalies from the former dataset. As a result, a
166 0.02°x0.02° grid of gravity anomalies on the land is obtained.

167 To concatenate the land and marine gravity anomaly data, 1'x1' gravity anomalies in the ocean
168 are clipped (or separated) from the complete SCRIPPS dataset, i.e., on both ocean and land. It is then
169 block averaged to the 0.02°x0.02° grid and is superimposed with the land gravity anomaly grid. The
170 former values were replaced by the latter at overlapping nodes to obtain the 0.02°x0.02° grid of the
171 merged gravity anomalies. Figure 2 shows the merged free-air gravity anomaly map. To check for
172 any discontinuities at the edges of the merged datasets, we computed and plotted the arctangent
173 (Figure 3a) and logarithmic (Figure 3b) values of the gradients of the merged data. We observe no
174 clear visual indication of any discontinuities at the boundaries of the merged data, but also partially
175 due to the ruggedness of the dataset in our study area that can be obscuring.

176 PLACE FIGURES 2 AND 3 NEAR HERE

177

178 **2.2 Digital Elevation Model**

179 The Digital Elevation Model (DEM) is another important input in geoid computation. It is mainly
180 used to compute the topographical effects (e.g., Forsberg 1984). Thus, a precise high-resolution DEM
181 should be used. We would like to mention here that DEM is generally used synonymously with a

182 Digital Surface Model (DSM) (e.g., SRTM, ASTER), but this should be avoided. Quantification of
183 the differences in the topographical effect with the use of DEM and DSM has been investigated by
184 Yang et al. (2019). Since India does not have a national DEM, therefore, after a DEM/DSM analysis
185 (Goyal et al. 2021a), it was decided to work with the best available DEM over India, i.e., the MERIT
186 3"x3" DEM (Yamazaki et al. 2017), for our computations. Though the accuracy of the MERIT DEM
187 varies considerably ($\pm$11.7 m to $\pm$47.3 m) over different landforms in India, an overall estimate for
188 the whole of India is $\pm$17.3 m (Goyal et al. 2021a).

189

190 **2.3 GNSS-Levelling**

191 India has different horizontal and vertical control networks. Therefore, presently there are only a
192 limited number of ground control points where we have the geodetic coordinates (latitude, longitude,
193 ellipsoidal heights) and levelled heights. Moreover, due to several restrictions on the datasets, only a
194 few of these available data points were available to us (Figure 4). The datasets in the Uttar Pradesh
195 west (UP west) and Uttar Pradesh east (UP east) regions were procured from SoI, while the datasets
196 over Hyderabad and Bangalore have been retrieved from Mishra (2018), who also used the SoI
197 dataset. According to Mishra (2018), horizontal and vertical precisions of GNSS data are within ±12
198 mm to ±26 mm and ±31 mm to ±53 mm, respectively. The vertical precision of the levelling heights
199 is not known to us, but they are from the high precision first level net of India. These heights are from
200 the Indian Vertical Datum 1909 (Burrard, 1910) and are based on the normal-orthometric height
201 system, while those on Indian Vertical Datum 2009 (G&RB 2018) are based on Helmert's
202 orthometric height system. We have not been provided with a clear indication on which heights have
203 been provided to us, and therefore, due to this anonymity of the height system, we consider the
204 levelling heights to be in the normal-orthometric height system (Jekeli 2000; Featherstone and Kuhn
205 2006).

206 PLACE FIGURE 4 NEAR HERE

3. METHODOLOGY AND RESULTS

An overview of the CUT methodology for computing the geoid undulations is shown by a flowchart in Figure 5. The CUT method primarily computes the quasigeoid using the analytical continuation solution (Moritz 1971; 1980) of Molodensky's problem (Molodensky et al. 1962). Moritz (1971) showed that Molodenksy's G_1 term can be approximated by the planar terrain correction (TC), which also needs an additional term that is equal to the first-order indirect effect (FOIE). We could not adopt the full CUT method-based reconstruction of Faye anomalies (Featherstone and Kirby 2000) because we already have gridded data, whereas CUT grids point Bouguer anomalies. Instead, we added the block averaged 0.02˚×0.02˚ grid of TCs (Figure 6a) to the free-air gravity anomaly grid to calculate area-mean Faye anomalies (Figure 6b). The block-averaged 0.02˚×0.02˚ TC grid was constructed from the 3"×3" TC grid computed with the MERIT DEM using the Optimal Separating Radius (OSR) in the spatial-spectral combined method suggested by Goyal et al. (2020). This method of TC guarantees the full convergence of the TC solution, i.e., down to <1μGal.

PLACE FIGURE 5 NEAR HERE

A different approach is used in the CUT method to apply ellipsoidal correction. Unlike other geoid computation strategies considered (UNB or KTH; cf. Huang et al. 2003; Ellmann 2005), the CUT method computes ellipsoidal area-mean free-air gravity anomalies on the topography using a Global Geopotential Model (GGM) (Featherstone et al. 2018). These are subtracted from the mean Faye gravity anomalies to obtain residual gravity anomalies (Figure 6c), which are then Stokes-integrated with the Featherstone-Evans-Olliver (FEO) modified kernel (Featherstone et al. 1998) to obtain the residual height anomalies. The FEO kernel, a deterministic modifier, is the combination of the Meissel (1971) and Vaníček and Kleusberg (1987) modifiers that simultaneously reduces the truncation error and improves the rate of convergence to zero of the series expansion of the truncation error (cf. Featherstone et al. 1998, Featherstone 2003). Additionally, the spherical reference radius in

232 the Stokes integration is set equal to the geocentric ellipsoidal radius of the computation point, and
233 this negates the need for further ellipsoidal corrections to Stokes's integral (Claessens 2006).

234 The residual height anomalies were computed using the following parameter-sweeps of the
235 modification degree (M): 0, 40, 80, 120, 160, 200, 240, 280, 300 and integration cap radius (ψ): 0.2°,
236 0.5°, 0.75°, 1°, 1.5°, 2° (e.g., Figure 6d for M=80, ψ=1.5°). The reference height anomalies on the
237 topography are computed using GGMs with a zero-degree term $\left(N_0\right)$ from the generalised Bruns's
238 formula (Eqn. 9) (Heiskanen and Moritz 1967) calculated for each latitude parallel, which are added
239 to the residual height anomalies to obtain the required height anomalies. An inconsistent use of Eqn.
240 9 can cause an error of ~1 m in the computed geoid undulations/height anomalies. We used normal
241 potential $U_0\left(=62636860.85\,m^2s^{-2}\right)$ from GRS80 (Moritz 2000) and the geopotential
242 $W_0\left(=62636853.4\,m^2s^{-2}\right)$ from IHRS (Sanchez et al., 2016).

243 $$N_0=\frac{GM_G-GM_E}{r\gamma_0}-\frac{W_0-U_0}{\gamma_0} \tag{9}$$

244 As a small modification to the original CUT method, we added the $FOIE=-\frac{\pi G\rho H^2}{\gamma}$ (Moritz, 1980,
245 Eqn. 48-29; Heiskanen and Moritz 1967, chapter 8) to the computed height anomalies. We note that
246 the negative sign is sometimes omitted (e.g., Sjöberg 2000; Hwang et al. 2020).

247 PLACE FIGURE 6 NEAR HERE

248 The geoid undulations are calculated by adding the quasigeoid-geoid separation term (Figure
249 6e; Flury and Rummel 2009) to the height anomalies. The more rigorous quasigeoid-geoid separation
250 term from Flury and Rummel (2009) differs quite considerably from the approximate formula given
251 in Heiskanen and Moritz (1967, p 328). The difference in the quasigeoid-geoid separation term from
252 the two methods is shown in Figure 6f. Acknowledging that the number and distribution of the
253 GNSS/levelling data points are not sufficient for reliable fitting (Kotsakis and Sideris 1999;

254 Fotopoulos 2003), we have not presented hybrid geoid and hybrid quasigeoid models for this
255 experiment over India.

256 The geoid should be validated with orthometric (Helmert or rigorous (Santos et al. 2006))
257 heights and the quasigeoid validated with normal heights. A more rigorous validation approach would
258 be to convert the normal-orthometric heights to Helmert's orthometric height and normal heights for
259 validating geoid and quasigeoid, respectively. Examples of this are Foroughi et al. (2017) and Janák
260 et al. (2017) over Auvergne, France, where normal heights were converted to rigorous heights for
261 validation of their developed geoid models. However, Indian levelled heights are based on the
262 normal-orthometric height system for which there is no specific choice of reference surface, i.e.,
263 either geoid or quasigeoid. Therefore, we are only able to "validate" the developed geoid and
264 quasigeoid models with the Indian normal-orthometric heights on an uncertain vertical datum
265 (Section 2.3).

266 Absolute and relative testing (Featherstone 2001) of both height anomalies and geoid
267 undulations are done in this study. The absolute testing is realised through point-wise subtraction of
268 gravimetric geoid undulations obtained using Stokesian integration (N) and the geometrical geoid
269 undulation (h - H) obtained using GNSS/levelling data (Eqn. 10).

270 $$\varepsilon_i^{abs} = N_i - \left(h_i - H_i\right) \quad \forall\, i = 1,2,3,.....n \tag{10}$$

271 where n is the total number of discrete GNSS/levelling data points. It is important to acknowledge
272 that absolute accuracy is only an assumption. This is principally because the levelled heights that
273 refer to the local vertical datum are not necessarily coincident with the geoid. This has been discussed
274 in detail by Featherstone (2001). The descriptive statistics of ε_i^{abs} are in Table 1.

275 PLACE TABLE 1 NEAR HERE

The relative testing of geoid and quasigeoid (Eqn. 11) is an analysis tool to investigate their gradients. This type of analysis is of more interest to land surveyors who use relative GNSS baselines and a geoid/quasigeoid gradients as a replacement for the more time-consuming differential levelling.

$$\varepsilon_{ij}^{rel} = \Delta N_{ij} - \left(\Delta h_{ij} - \Delta H_{ij}\right) \quad \forall i, j = 1, 2, 3, \ldots\ldots n; i \neq j \tag{11}$$

The descriptive statistics of ε_{ij}^{rel}), and the ratio of mean differences to the mean baseline length in parts per million (average ppm in mm/km) for the geoid and quasigeoid are in Table 2.

PLACE TABLE 2 NEAR HERE

The variation of standard deviation in the Indian geoid and quasigeoid models, on testing with GNSS/levelling data, for different combinations of modification degree and integration cap are shown in Figures 7a and 7b, respectively. Table 1 depicts the region-wise (UP west, UP east, Hyderabad, Bangalore, and all together) descriptive statistics for the geoid and quasigeoid for the combination of M=80 and ψ=1.5°. Though the standard deviation for the whole of India is smaller with the combination of M=40 and ψ=1.5° compared to M=80 and ψ=1.5° (cf. Figure 7), standard deviations for the four individual regions are less than or equal to the combination of M=80 and ψ=1.5° compared to M=40 and ψ=1.5°. Therefore, M=80 and ψ=1.5° was chosen to present our results. The results of the relative testing are shown in Figures 8a and 8b, and Table 2. The computed Indian gravimetric geoid (IndGG-CUT2021) and corresponding contours (at a 2 m contour interval) are shown in Figures 9a and 9b, respectively.

PLACE FIGURES 7, 8 AND 9 NEAR HERE

4. DISCUSSION, RECOMMENDATIONS AND CONCLUSIONS

Though the number (119) and the distribution (Figure 4) of the GNSS/levelling data points are insufficient to draw concrete conclusions about the quality of the computed gravimetric geoid and quasigeoid models, the following are some major observations from our experimental results:

1. Since the study area comprises the most complex topography varying from the Himalayas to the Gangetic plains and a long peninsular coastline, Figure 6 possibly depicts the extreme (maximum and minimum) values of planar TC, Faye gravity anomaly, and quasigeoid-geoid separation on the planet.

2. From the viewpoint of the "cm-level accurate" geoid, Figure 6f suggests that a more rigorous method (e.g., Flury and Rummel 2009) should be preferred for calculating the quasigeoid-geoid separation over a simple approximate formula (e.g., Heiskanen and Moritz 1967). There exist other formulas for the quasigeoid-geoid separation term (e.g., Sjöberg 2010; Foroughi and Tenzer 2017), but they are not tested here.

3. Figures 7 suggest that the FEO kernel (Featherstone et al. 1998) is not numerically unstable for higher modification degrees, as shown in Featherstone (2003), Li and Wang (2011), Featherstone et al. (2018) and Claessens and Filmer (2020). However, this observation can also result from our choice of parameter sweeps and limited datasets for validation, thus requiring further investigation.

4. Generally, standard deviations versus GNSS/levelling are large for lower modification degrees and larger integration radii (Featherstone et al. 2018; Claessens and Filmer 2020). However, Figure 7 shows an opposite trend in India, with smaller standard deviations for lower modification degrees and larger integration radii. This is primarily attributable to the north-south tilt in the India height datum (cf. Table 1). However, he smaller number of GNSS/levelling data and their poor distribution are also likely to contribute to this observation.

5. Figure 7 shows that the Indian levelling heights are marginally better referred to the quasigeoid (std = $\pm$0.389 m) than the geoid (std = $\pm$0.396 m). However, Table 1 shows that the geoid has an equal or better precision estimate than the quasigeoid (in terms of standard deviation) in each of the four regions individually. The difference in the standard deviations of the quasigeoid and geoid comparison for the whole of India seems to be a consequence, mostly, of the smaller mean

of the quasigeoid (0.690 m) than the geoid (0.751 m) comparison over Bangalore. Also, with the given precision estimate of the data points, there can yet be no preferred choice between geoid or quasigeoid for the Indian vertical datum. Hence, a larger set of data points are needed for any possible claim of reference surface for India. Though the overall standard deviation of the computed geoid/quasigeoid (Table 1) is ~±0.40 m, it varies from ~±0.03 m to ~±0.16 m if only evaluated individually in the four small test regions.

6. Table 2 indicates that the largest misclosures in Figure 8 are probably due to the tilt in the Indian height datum and the relative closeness of data points in Hyderabad and Bangalore, which also explains the larger ppm values found in those regions. Spikes in Figures 8a and 8b at distances of approximately [0-50] km, [450-550] km, [900-1200] km, and [1200-1900] km are due to the errors and differences (north-south tilt) in the baselines for [Bangalore and Hyderabad, individually], [Bangalore to Hyderabad], [UP west, UP east to Hyderabad], and [UP west, UP east to Bangalore], respectively.

7. On comparison of validations of the Indian gravimetric geoid with the CUT method and the GGM (Table 3), it is observed that though the overall mean values are improved for all regions except Bangalore, an improvement in the standard deviation beyond $\pm$0.01 m is observed only for UP east. However, the standard deviation of gravimetric geoid in UP west is degraded by $\pm$0.03 m as compared to the EIGEN-6C4. A degradation in the standard deviation of the gravimetric geoid is also observed in Featherstone and Sideris (1998). This was, and similarly is, attributed to errors in either one or more of terrestrial gravity data, GGMs and the GNSS/levelling data.

   There is little to no improvement with the inclusion of the terrestrial gravity data with the CUT method because it makes use of the highest available degree-order GGMs. Also, the GETECH data is possibly already included in the high degree-order GGM (e.g., EGM2008, Pavlis et al., 2012; 2013)

8. The Faye gravity anomaly (Figure 6b), geoid (Figure 9a), and contour map (Figure 9b) somewhat depict the separation line of the Indian and the Eurasian plate. Thus, the results presented in this study could be important for geophysical studies. The contour pattern around the location of 24˚N and 82˚E seems intriguing for some gravimetric studies in that region. It should also be noted that the area comprises one of the largest coalfields of India with the thickest and different varieties of coal seams.

As a final remark, first experimental geoid and quasigeoid models for India have been computed with a standard deviation of ±0.396 m and ±0.389 m, respectively, with respect to a small number of test regions. However, for the four regions individually, the standard deviation varies from ±0.030 m to ±0.158 m for the geoid and ±0.032 m to ±0.158 m for the quasigeoid. Though all the results presented herein are the first from India, the geoid/quasigeoid must be improved with dense, precise gravity data. Moreover, a larger number of GNSS/levelling data points must become available for more rigorous validation of the gravimetric geoid/quasigeoid. For the re-computation of the Indian geoid/quasigeoid with the CUT method and additional gravity data, the TC and the quasigeoid-geoid separation term need not be computed again unless a high-resolution and more precise DEM is available. Further, due to the complexities of the Indian topography and geomorphic characteristics, other geoid/quasigeoid computation strategies should also be tested over India.

Acknowledgments

We are thankful to the GETECH Pty. Ltd. and the Survey of India for providing the gravity data and GNSS/levelling data, respectively. The Indian SPARC scheme is thanked for providing partial funding to procure the GETECH gravity data. The National Centre for Geodesy, established at Indian Institute of Technology Kanpur, is duly thanked for partial funding to procure the GETECH gravity data, and full funding for a) procurement of the GNSS/levelling data and b) the additional page

373 charges for this article. We are also thankful to the three anonymous reviewers and the editor (X. Li)
374 for their prompt and constructive comments on an earlier version of this manuscript.

375

376 **References**

377 Ågren, J., 2004: Regional geoid model determination methods for the era of satellite gravimetry. (Numerical
378 investigations using synthetic earth gravity models). PhD Thesis, KTH University, Stockholm, Sweden.

379 Burrard, S., 1910: Levelling of precision in India. The Great Trigonometrical Survey of India, Vol XIX. Survey
380 of India, Dehradun, India.

381 Carrion, D., N. Kumar, R. Barzaghi, A. P. Singh, and B. Singh, 2009: Gravity and geoid estimate in south
382 India and their comparison with EGM2008. Newton's Bulletin, **4**, 275–283.

383 Catalao, J., 2006: Iberia-Azores Gravity Model (IAGRM) using multi-source gravity data. Earth Planet Sp.,
384 **58**, 277–286, doi: 10.1186/BF03351924

385 Claessens, S. J., 2006: Solutions to ellipsoidal boundary value problems for gravity field modelling. PhD
386 thesis, Curtin University, Perth, Australia

387 Claessens, S. J., and M. S. Filmer, 2020: Towards an International Height Reference System: insights from
388 the Colorado geoid experiment using AUSGeoid computation methods. J. Geod., **94**, 52, doi:
389 10.1007/s00190-020-01379-3

390 Ecker, E. and E. Mittermayer, 1969: Gravity corrections for the influence of the atmosphere. Boll. Goefis.
391 Teor. Appl., **11**, 7080.

392 Ellmann, A. and P. Vaníček, 2007: UNB application of Stokes–Helmert's approach to geoid computation. J.
393 Geodyn., **43**, 200–213, doi: 10.1016/j.jog.2006.09.019

394 Ellmann, A., 2005: A Numerical Comparison of Different Ellipsoidal Corrections to Stokes' Formula, In:
395 Sansò, F. (Ed.), A Window on the Future of Geodesy, International Association of Geodesy Symposia
396 128. Springer-Verlag, Berlin,Heidelberg, pp. 409–414, doi: 10.1007/3-540-27432-4_70

397 Featherstone, W. E., 2000: Refinement of gravimetric geoid using GPS and leveling data. J. Surv. Eng., **126**,
398 27–56, doi: 10.1061/(ASCE)0733-9453(2000)126:2(27)

399 Featherstone, W. E., 2001: Absolute and relative testing of gravimetric geoid models using Global Positioning
400 System and orthometric height data. Comput. Geosci., **27**, 807–814, doi: 10.1016/S0098-3004(00)00169-
401 2

Featherstone, W. E., 2003: Software for computing five existing types of deterministically modified integration kernel for gravimetric geoid determination. Comput. Geosci., **29**, 183–193, doi: 10.1016/S0098-3004(02)00074-2

Featherstone, W. E., J. F. Kirby, C. Hirt, M. S. Filmer, S. J. Claessens, N. J. Brown, G. Hu, and G. M. Johnston, 2011: The AUSGeoid09 model of the Australian height datum. J. Geod., **85**, 133–150, doi: 10.1007/s00190-010-0422-2

Featherstone, W. E., J. F. Kirby, A. H. W. Kearsley, J. R. Gilliland, G. M. Johnston, J. Steed, R. Forsberg, and M. G. Sideris, 2001: The AUSGeoid98 geoid model of Australia: data treatment, computations and comparisons with GPS-levelling data. J. Geod., **75**, 313–330, doi: 10.1007/s001900100177

Featherstone, W. E., J. C. McCubbine, N. J. Brown, S. J. Claessens, M. S. Filmer, and J. F. Kirby, 2018: The first Australian gravimetric quasigeoid model with location-specific uncertainty estimates. J. Geod., **92,** 149–168, doi: 10.1007/s00190-017-1053-7

Featherstone, W., J. Evans, and J. Olliver, 1998: A Meissl-modified Vaníček and Kleusberg kernel to reduce the truncation error in gravimetric geoid computations. J. Geod., **72**, 154-160, doi: 10.1007/s001900050157

Featherstone, W. E. and M. Kuhn, 2006: Height systems and vertical datums: a review in the Australian context. J. Spat. Sci., **51**, 21-41, doi: 10.1080/14498596.2006.9635062

Featherstone, W. E. and M. G. Sideris, 1998: Modified kernels in spectral geoid determination: first results from Western Australia, In: Forsberg, R., M. Feissel and R. Dietrich (Eds.), Geodesy on the move, International Association of Geodesy Symposia 119. Springer, Berlin, Heidelberg, pp. 188-193, doi: 10.1007/978-3-642-72245-5_26

Featherstone, W. E. and M. S. Filmer, 2012: The north-south tilt in the Australian Height Datum is explained by the ocean's mean dynamic topography. J. Geophys. Res., **117**, C08035, doi: 10.1029/2012JC007974

Featherstone, W. E. and J. F. Kirby, 2000: The reduction of aliasing in gravity anomalies and geoid heights using digital terrain data. Geophys. J. Int., **141**, 204–212, doi: 10.1046/j.1365-246X.2000.00082.x

427 Fischer, I., 1961: The present extent of the astro-geodetic geoid and the geodetic world datum derived from it.
428 Bull. Geodesique, **61**, 245–264, doi: 10.1007/BF02854151

429 Fischer, I., 1975: Does mean sea level slope up or down toward north? Bull. Geodesique, **115**, 17–26, doi:
430 10.1007/BF02523939

431 Fischer, I., 1977: Mean sea level and the marine geoid - an analysis of concepts. Mar. Geod., **1**, 37–59, doi:
432 10.1080/01490417709387950

433 Flury, J. and R. Rummel, 2009: On the geoid–quasigeoid separation in mountain areas. J. Geod., **83**, 829–847,
434 doi: 10.1007/s00190-009-0302-9

435 Foroughi, I. and R. Tenzer, 2017: Comparison of different methods for estimating the geoid-to-quasi-geoid
436 separation. Geophys. J. Int., **210**, 1001–1020, doi: 10.1093/gji/ggx221

437 Foroughi, I., P. Vaníček, M. Sheng, R. W. Kingdon, M. C. Santos, 2017: In defense of classical height system.
438 Geophys. J. Int., **211**, 1154-1161, doi: 10.1093/gji/ggx366

439 Forsberg, R., 1984: Study of terrain reductions, density anomalies and geophysical inversion methods in
440 gravity field modelling. Reports of the Department of Geodetic Science and Surveying, No. 355. The Ohio
441 State University, Colombus, Ohio.

442 Forsberg, R., 1985: Gravity field terrain effect computations by FFT. Bull. Geodesique, **59**, 342–360, doi:
443 10.1007/BF02521068

444 Forsberg, R., 1998: The use of spectral techniques in gravity field modelling: Trends and perspectives. Phys.
445 Chem. Earth, **23**, 31–39, doi: 10.1016/S0079-1946(97)00238-3

446 Forsberg, R., Tscherning, C.C., 2008: An overview manual for the GRAVSOFT geodetic gravity field
447 modelling programs. https://ftp.space.dtu.dk/pub/RF/gravsoft_manual2014.pdf

448 Fotopoulos, G., 2003: An analysis on the optimal combination of geoid, orthometric and ellipsoidal height
449 data. PhD Thesis, University of Calgary, Canada.

450 G&RB, 2018: Report on redefinition of Indian Vertical Datum IVD2009. Geodetic and Research Branch,
451 Survey of India, Dehradun, India.

452 GETECH, 2006: Gravity data compilation of India. Report no. G0610, University of Leeds, United Kingdom.

453 Goyal, R., B. Nagarajan, and O. Dikshit, 2017: Status of precise geoid modelling in India: A review. In:
454 Proceedings of 37th INCA International congress on Geoinformatics for Carto-Diversity and Its
455 Management. Indian Cartographer, pp. 308-313. ISSN 0927-8392

456 Goyal, R., W. E. Featherstone, O. Dikshit, and N. Balasubramania, 2021a: Comparison and Validation of
457 Satellite-Derived Digital Surface/Elevation Models over India. J. Indian. Soc. Remote. Sens., **49**, 971–
458 986, doi: 10.1007/s12524-020-01273-7

459 Goyal, R., W. E. Featherstone, D. Tsoulis, and O. Dikshit, 2020: Efficient spatial-spectral computation of local
460 planar gravimetric terrain corrections from high-resolution digital elevation models. Geophys. J. Int., **221**,
461 1820–1831, doi: 10.1093/gji/ggaa107

462 Goyal, R., J. Ågren, W. E. Featherstone, L. E. Sjöberg, O. Dikshit, and N. Balasubramanian, 2021b: Empirical
463 comparison between stochastic and deterministic modifiers over the French Auvergne geoid computation
464 test-bed. Surv. Rev., Online first. doi: 10.1080/00396265.2021.1871821

465 Hackney, R. I. and W. E. Featherstone, 2003: Geodetic versus geophysical perspectives of the 'gravity
466 anomaly'. Geophys. J. Int., **154**, 35-43, doi: 10.1046/j.1365-246X.2003.01941.x

467 Heiskanen, W.A. and H. Moritz, 1967: Physical geodesy, San Francisco and London: W H Freeman and Co.

468 Huang, J., M. Veronneau, and S. D. Pagiatakis, 2003: On the ellipsoidal correction to the spherical Stokes
469 solution of the gravimetric geoid. J. Geod., **77**, 171–181, doi: 10.1007/s00190-003-0317-6

470 Hwang, C., H.-J. Hsu, W. E. Featherstone, C.-C. Cheng, M. Yang, W. Huang, C.-Y. Wang, J.-F. Huang, K.-
471 H. Chen, C.-H. Huang, H. Chen, and W.-Y. Su, 2020: New gravimetric-only and hybrid geoid models of
472 Taiwan for height modernisation, cross-island datum connection and airborne LiDAR mapping. J. Geod.,
473 **94**, 83, doi: 10.1007/s00190-020-01412-5

474 Janák, J., P. Vaníček, I. Foroughi, R. Kingdon, M. B. Sheng, M. C. Santos, 2017: Computation of precise
475 geoid model of Auvergne using current UNB Stokes-Helmert's approach. Contributions to geophysics and
476 geodesy, **47**, 201-229, doi: 10.1515/congeo-2017-0011

477 Jekeli, C., 2000: Heights, the Geopotential, and Vertical Datums. Report 459, Department of Civil and
478 Environmental Engineering and Geodetic Science, Ohio State University, Columbus, Ohio, USA.

Kotsakis, C., and M. Sideris, 1999: On the adjustment of combined GPS/levelling/geoid networks. J. Geod., **73**, 412-421, doi: 10.1007/s001900050261

Li, X. and Y. Wang, 2011: Comparisons of geoid models over Alaska computed with different Stokes' kernel modifications. J. Geod. Sci., **1**, 136-142, doi: 10.2478/v10156-010-0016-1

Li, X., 2018: Using radial basis functions in airborne gravimetry for local geoid improvement. J. Geod., **92**, 471–485, doi: 10.1007/s00190-017-1074-2

LINZ, 2016: New Zealand Quasigeoid 2016 (NZGeoid2016). Retrieved from: https://www.linz.govt.nz/data/geodetic-system/datums-projections-and-heights/vertical-datums/new-zealand-quasigeoid-2016-nzgeoid2016. Accessed on: 21-04-2021

Liu, Q., M. Schmidt, L. Sánchez, and M. Willberg, 2020: Regional gravity field refinement for (quasi-) geoid determination based on spherical radial basis functions in Colorado. J. Geod., **94**, 99, doi: 10.1007/s00190-020-01431-2

Macomber, M. M., 1984: World Geodetic System 1984. Defense Mapping Agency, Washington D.C., United States of America. https://ia800108.us.archive.org/20/items/DTIC_ADA147409/DTIC_ADA147409.pdf

McCubbine, J.C., V. Stagpoole, F. Caratori Tontini, M. Amos, E. Smith, R. Winefield, 2017: Gravity anomaly grids for the New Zealand region. New Zealand Journal of Geology and Geophysics, **60**, 381–391, doi: 10.1080/00288306.2017.1346692

Meissl, P., 1971: Preparations for the numerical evaluation of second-order Molodensky-type formulas. OSU Report 163, Department of Geodetic Science, Ohio State University, Columbus

Mishra, U.N., 2018: A comparative evaluation of methods for development of Indian geoid model. PhD thesis, IIT Roorkee, India

Mishra, U. N. and J. K. Ghosh, 2016: Development of a gravimetric geoid model and a comparative study. GAC, **42**, 75–84, doi: 10.3846/20296991.2016.1226368

Molodensky, M. S., V. F. Eremeev, and M. I. Yurkina, 1962: Methods for study of the external gravity field and figure of the Earth. Israel Program for Scientific Translations, Jerusalem, Israel.

504 Moritz, H., 1980: Advanced physical geodesy, Advances in Planetary Geology, Abacus Press, Tunbridge,
505 England.

506 Moritz, H., 2000: Geodetic Reference System 1980. J. Geod., **74**, 128–133, doi: 10.1007/s001900050278

507 Moritz, H., 1971: Series solutions of Molodensky's problem. Deutsche Geodaetische Kommission Bayer.
508 Akad. Wiss., 70.

509 NGS, 2017: Blueprint for 2022, Part 2: Geopotential coordinates. NOAA Technical Report NOS NGS 64.
510 https://geodesy.noaa.gov/PUBS_LIB/NOAA_TR_NOS_NGS_0064.pdf

511 NGS 2019: Blueprint for modernized NSRS, Part 3: working in the modernized NSRS, NOAA Technical
512 Report NOS NGS 67. https://www.ngs.noaa.gov/PUBS_LIB/NOAA_TR_NOS_NGS_0067.pdf

513 Olesen, A.V., O. B. Andersen, and C. C. Tscherning, 2002: Merging of Airborne Gravity and Gravity Derived
514 from Satellite Altimetry: Test Cases Along the Coast of Greenland. Stud. Geophys. Geod., **46**, 387–394,
515 doi: 10.1023/A:1019577232253

516 Pavlis, N. K., S. A. Holmes, S. C. Kenyon, and J. K. Factor, 2012: The development and evaluation of the
517 Earth Gravitational Model 2008 (EGM2008). J. Geophys. Res.: Solid Earth, **117**, B04406, doi:
518 10.1029/2011JB008916

519 Pavlis, N. K., S. A. Holmes, S. C. Kenyon, and J. K. Factor, 2013: Correction to "The development and
520 evaluation of the Earth Gravitational Model 2008 (EGM2008)". J. Geophys. Res, **118**, 2633, doi:
521 10.1002/jgrb.50167

522 Sánchez, L., R. Čunderlík, N. Dayoub, K. Mikula, Z. Minarechová, Z. Šíma, V. Vatrt, and M. Vojtíšková,
523 2016: A conventional value for the geoid reference potential W_0. J. Geod., **90**, 815–835, doi:
524 10.1007/s00190-016-0913-x

525 Sandwell, D. T., H. Harper, B. Tozer and W. H. F. Smith, 2019: Gravity field recovery from geodetic altimeter
526 missions. Adv. Space Res., **68**, 1059-1072, doi: 10.1016/j.asr.2019.09.011

527 Santos, M. C., P. Vaníček, W. E. Featherstone, R. Kingdon, A. Ellmann, B.-A. Martin, M. Kuhn, and R.
528 Tenzer, 2006: The relation between rigorous and Helmert's definitions of orthometric heights. J. Geod.,
529 **80**, 691–704, doi: 10.1007/s00190-006-0086-0

Singh, S. K., 2007: Development of high-resolution gravimetric geoid model for central India. PhD Thesis, Indian Institute of Technology Roorkee, India.

Singh, S. K., 2018: Towards a new vertical datum for India. in: FIG Congress 2018, Istanbul, Turkey. https://fig.net/resources/proceedings/fig_proceedings/fig2018/papers/ts06e/TS06E_singh_9497.pdf

Singh, S. K. and R. Srivastava, R., 2018: Development of geoid model-A case study on western India. in: FIG Congress 2018, Istanbul, Turkey. https://fig.net/resources/proceedings/fig_proceedings/fig2018/papers/ts06e/TS06E_singh_srivastava_9496.pdf

Sjöberg, L. E., 1984: Least squares modification of Stokes and Venning Meinesz formulas by accounting for errors of truncation, potential coefficients and gravity data. Technical Report 27, Department of Geodesy, Institute of Geophysics, University of Uppsala, Uppsala, Sweden.

Sjöberg, L. E., 1991: Refined least squares modification of Stokes' formula. manuscr. geod., **16**, 367–375.

Sjöberg, L. E., 2000: Topographic effects by the Stokes-Helmert method of geoid and quasi-geoid determinations. J. Geod., **74**, 255–268, doi: 10.1007/s001900050284

Sjöberg, L. E., 2003: A computational scheme to model the geoid by the modified Stokes formula without gravity reductions. J. Geod., **77**, 423–432, doi: 10.1007/s00190-003-0338-1

Sjöberg, L. E., 2010: A strict formula for geoid-to-quasigeoid separation. J. Geod., **84**, 699–702, doi: 10.1007/s00190-010-0407-1

Srinivas, N., V. M. Tiwari, J. S. Tarial, S. Prajapti, A. E. Meshram, B. Singh, and B. Nagarajan, 2012: Gravimetric geoid of a part of south India and its comparison with global geopotential models and GPS-levelling data. J. Earth. Syst. Sci., **121**, 1025–1032, doi: 10.1007/s12040-012-0205-7

Stokes, G. G., 1849: On the variation of gravity and the surface of the Earth. Cambridge Philosophical Society, Transactions, **8**, 672-695.

Strykowski G. and R. Forsberg, 1998: Operational Merging of Satellite, Airborne and Surface Gravity Data by Draping Techniques. In: Forsberg R., M. Feissel, and R. Dietrich (eds) Geodesy on the Move.

555 International Association of Geodesy Symposia 119. Springer, Berlin, Heidelberg, doi: 10.1007/978-
556 3-642-72245-5_35

557 UNB, 2002: SHGEO: Stokes – Helmert's GEOid software for precise geoid computation: Reference manual.
558 University of New Brunswick, Fredericton, Canada.
559 http://www2.unb.ca/gge/Research/GRL/GeodesyGroup/SHGeo/Manual/SHGeo_manual_I_2009.pdf

560 Vaníček, P. and Kleusberg, A., 1987: The Canadian geoid – Stokesian approach. manuscr. geod., **12**, 86-98.

561 Vaníček, P. and Z. Martinec, 1994: The Stokes-Helmert scheme for the evaluation of a precise geoid. manuscr.
562 geod., **19**, 119-128.

563 Vaníček, P., J. Huang, P. Novák, S. Pagiatakis, M. Véronneau, Z. Martinec, and W. E. Featherstone, 1999:
564 Determination of the boundary values for the Stokes-Helmert problem. J. Geod., **73**, 180–192, doi:
565 10.1007/s001900050235

566 Véronneau, M. and J. Huang, 2016: The Canadian Geodetic Vertical Datum of 2013 (CGVD2013).
567 Geomatica, **70**, 9–19, doi: 10.5623/cig2016-101

568 Yamazaki, D., D. Ikeshima, R. Tawatari, T. Yamaguchi, F. O'Loughlin, J. C. Neal, C. C. Sampson, S. Kanae,
569 and P. D. Bates, 2017: A high-accuracy map of global terrain elevations: Accurate Global Terrain
570 Elevation map. Geophys. Res. Lett., **44**, 5844–5853, doi: 10.1002/2017GL072874

571 Yang, M., C. Hirt, M. Rexer, R. Pail, and D. Yamazaki, 2019: The tree-canopy effect in gravity forward
572 modelling. Geophys. J. Int., **219**, 271–289, doi: 10.1093/gji/ggz264

573

574

Figure Legends

Figure 1: Error map of the SCRIPPSv28.1 marine gravity-anomaly data (units in mGal).

Figure 2: Merged gravity anomaly data from GETECH, EGM2008 (d/o 900) and SCRIPPS (units in mGal)

Figure 3: Arctangent (a) and logarithmic (b) plot of gradients of merged gravity anomaly data to attempt to identify discontinuities at the edges of the merged grids.

Figure 4: Spatial coverage of the available 119 GNSS/levelling data points

Figure 5: Flowchart of the CUT methodology of geoid/quasigeoid computation as applied in India for these experiments.

Figure 6: a) Block averaged planar TC, b) Faye anomaly, c) residual Faye anomaly, d) residual quasigeoid (M=80 and ψ=1.5˚), e) quasigeoid-geoid separation term (Flury and Rummel 2009), f) difference in quasigeoid-geoid separation term (Flury and Rummel 2009 minus Heiskanen and Moritz 1967). [*all on a 0.02˚×0.02˚ grid*] (units of a, b, c in mGal and d, e, f in m)

Figure 7: Standard deviation of a) geoid and b) quasigeoid of India for different combinations of modification degree and integration cap (units in m).

Figure 8: Magnitude of relative differences (blue circles) for the a) geoid, and b) quasigeoid. Orange and yellow circles represent the maximum permissible in-field misclose for Indian high-precision (k = 3) and double tertiary (k = 12) levelling for each baseline, respectively (units in m).

Figure 9: a) Indian gravimetric geoid computed using the CUT method (units in m), and b) corresponding 2 m geoid contours.

Illustrations

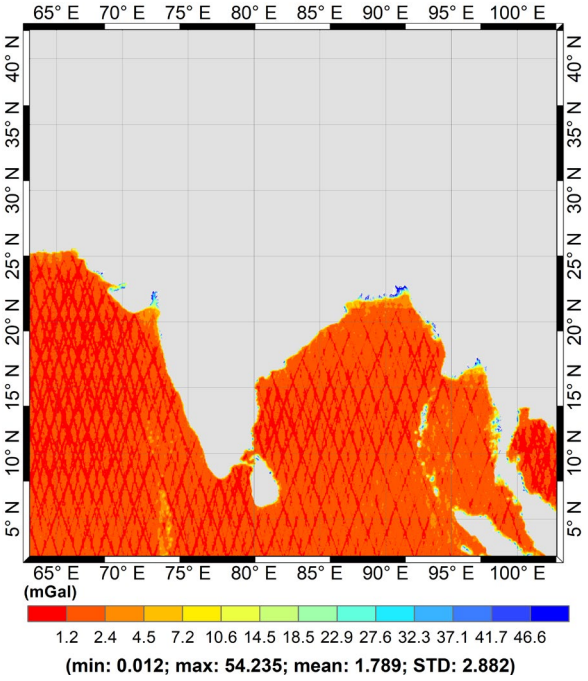

Figure 1: Error map of the SCRIPPSv28.1 marine gravity-anomaly data (units in mGal).

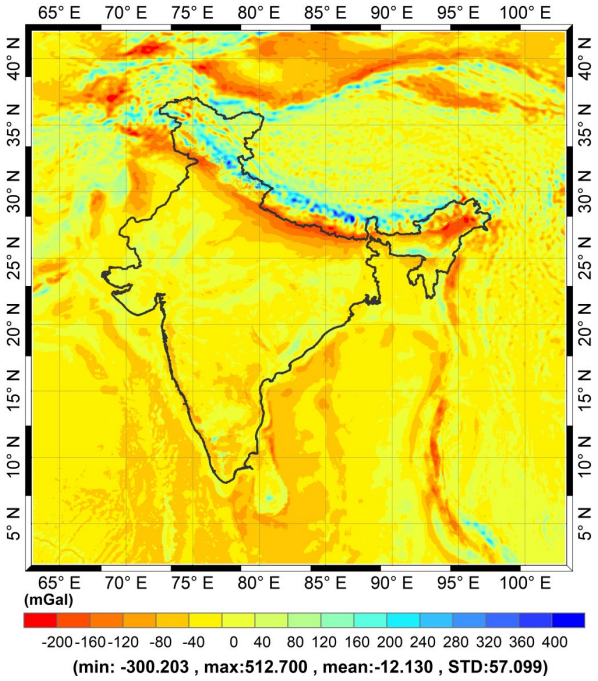

602 Figure 2: Merged gravity anomaly data from GETECH, EGM2008 (d/o 900) and SCRIPPS (units

603 in mGal)

604

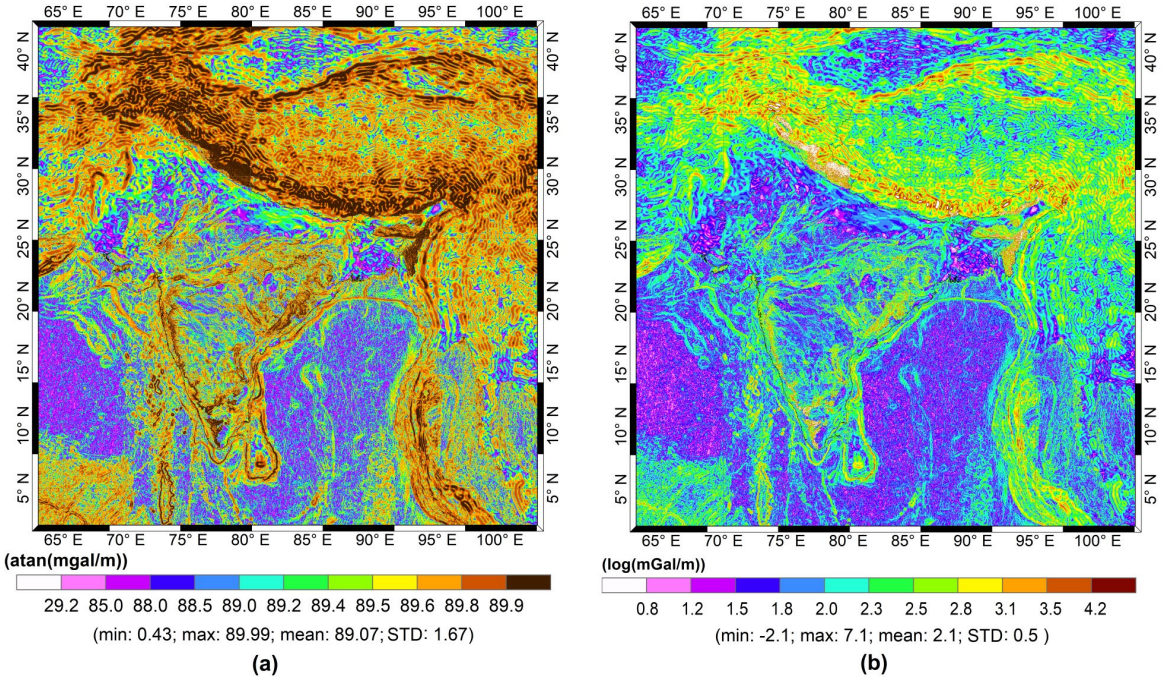

606 Figure 3: Arctangent (a) and logarithmic (b) plot of gradients of merged gravity anomaly data to

607 attempt to identify discontinuities at the edges of the merged grids.

608

609

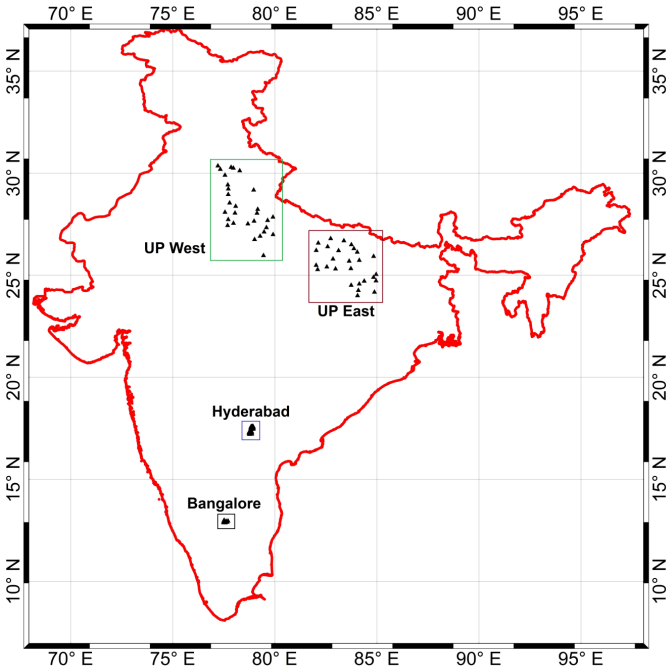

611 Figure 4: Spatial coverage of the available 119 GNSS/levelling data points

612

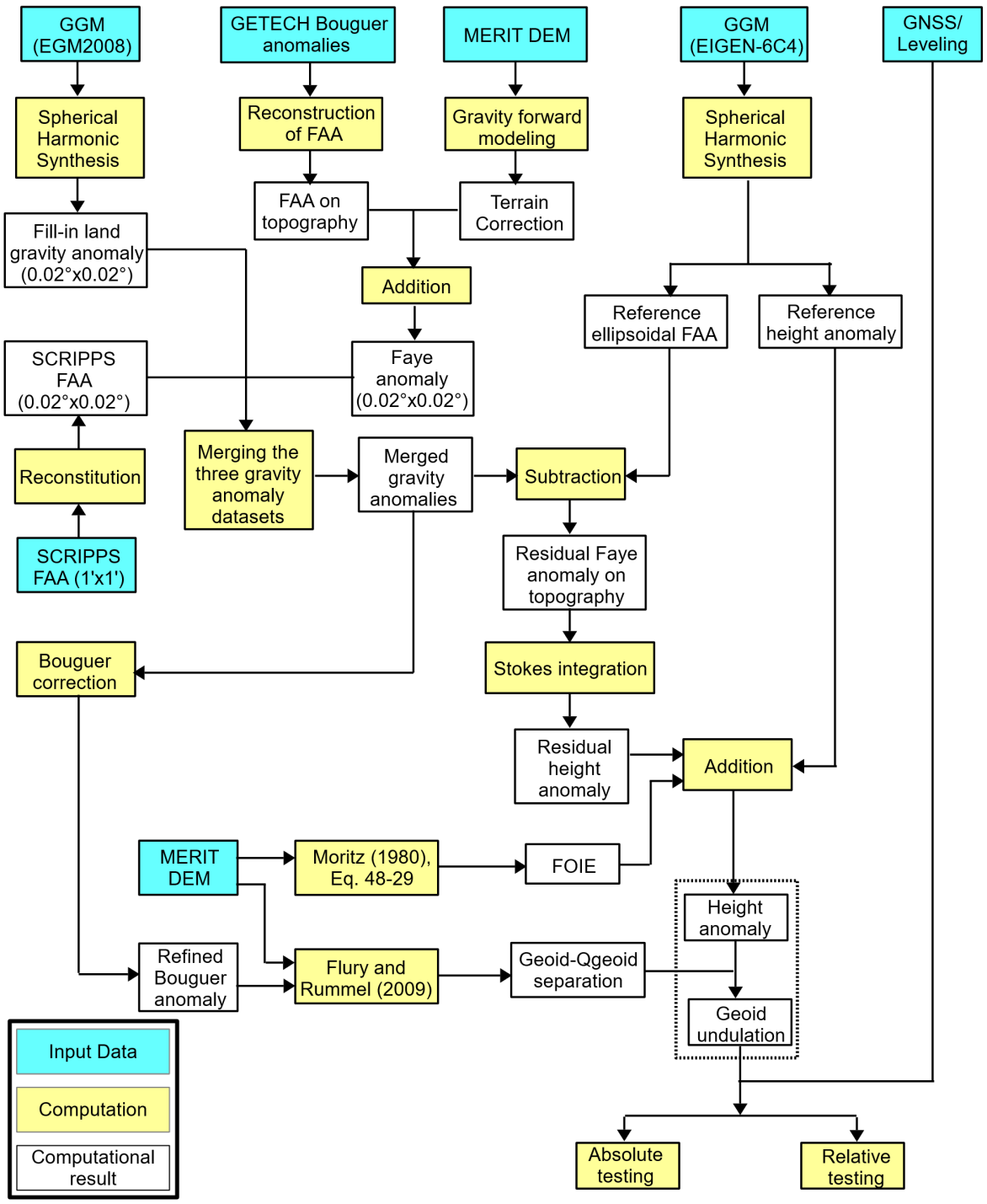

614 Figure 5: Flowchart of the CUT methodology of geoid/quasigeoid computation as applied in India

615 for these experiments.

616

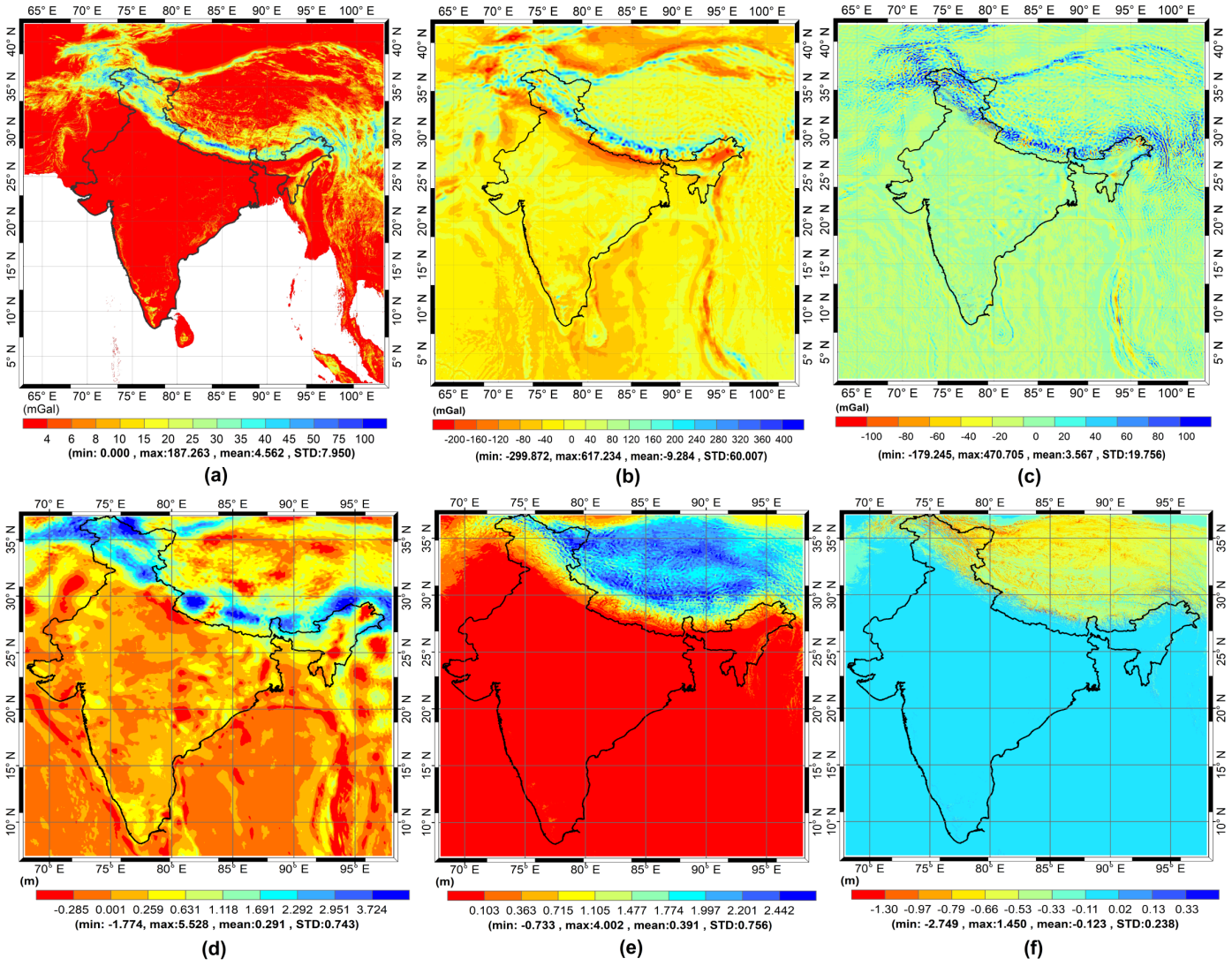

Figure 6: a) Block averaged planar TC, b) Faye anomaly, c) residual Faye anomaly, d) residual quasigeoid (M=80 and ψ=1.5˚), e) quasigeoid-geoid separation term (Flury and Rummel 2009), f) difference in quasigeoid-geoid separation term (Flury and Rummel 2009 minus Heiskanen and Moritz 1967). [*all on a 0.02˚×0.02˚ grid*] (units of a, b, c in mGal and d, e, f in m)

626

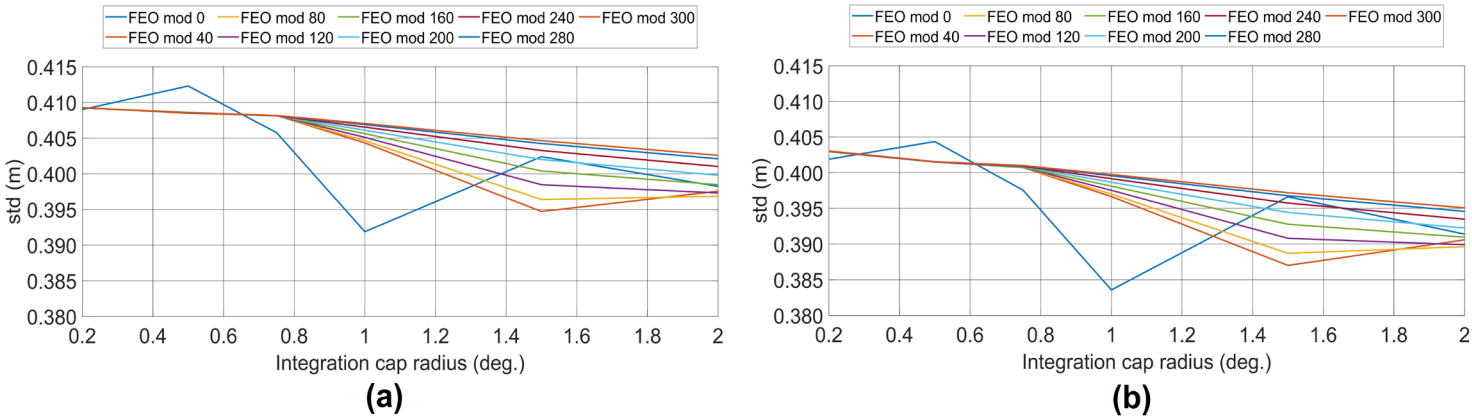

628 Figure 7: Standard deviation of a) geoid and b) quasigeoid of India for different combinations of

629 modification degree and integration cap (units in m).

630

631

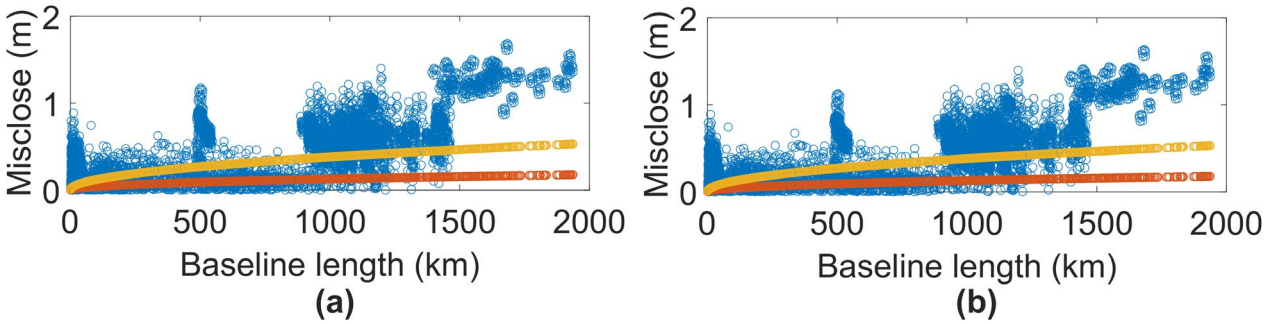

633 Figure 8: Magnitude of relative differences (blue circles) for the a. geoid, and b. quasigeoid. Orange
634 and yellow circles represent the maximum permissible in-field misclose for Indian high-precision (k
635 = 3) and double tertiary (k = 12) levelling for each baseline, respectively (units in m).

636

637

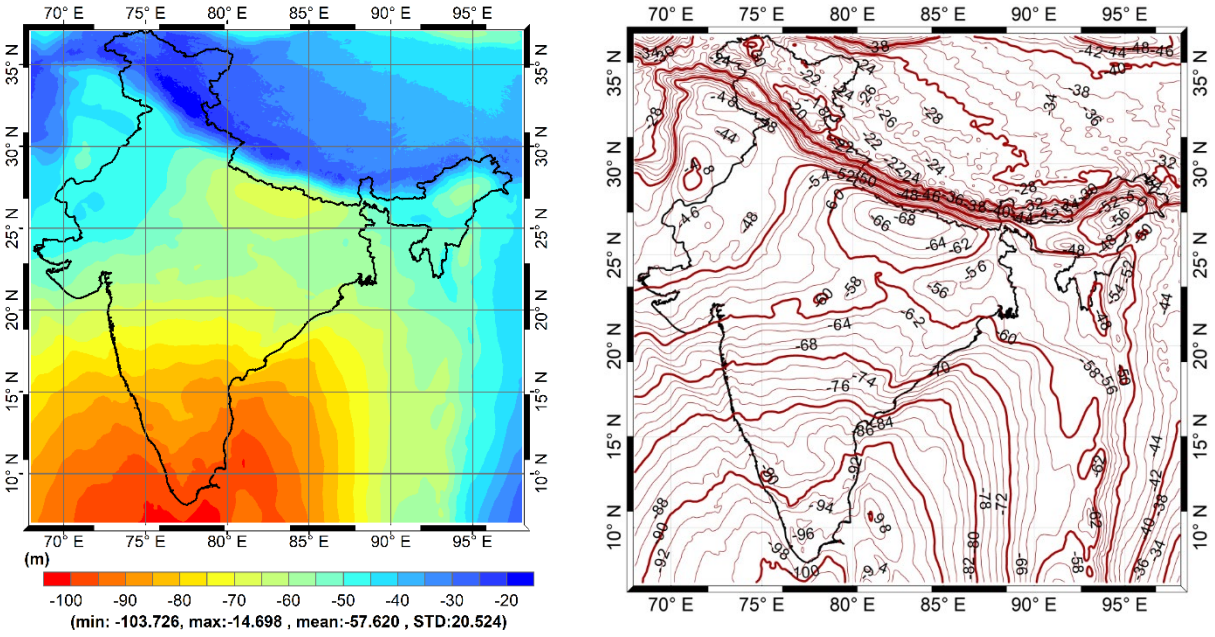

638

639 Figure 9: a) Indian gravimetric geoid computed using the CUT method (units in m), and b)
640 corresponding 2 m geoid contours.

641

642 # Tables

643 Table 1: Statistics for the region-wise geoid/quasigeoid (for M=80 and ψ=1.5˚) absolute testing (units in m)

Region	Geoid				Quasigeoid			
(no. of points)	min	max	mean	STD	Min	Max	Mean	STD
India (119)	-0.897	0.788	-0.171	±0.396	-0.906	0.726	-0.185	±0.389
UP west (29)	-0.897	-0.154	-0.532	±0.138	-0.906	-0.164	-0.548	±0.142
UP east (27)	-0.712	-0.338	-0.521	±0.114	-0.711	-0.340	-0.523	±0.114
Hyderabad (56)	-0.385	0.501	0.070	±0.158	-0.400	0.488	0.057	±0.158
Bangalore (7)	0.709	0.788	0.751	±0.030	0.645	0.726	0.690	±0.032

644

645

646

647 Table 2: Statistics for the region-wise geoid/quasigeoid (for M=80 and ψ=1.5˚) relative testing

Region	Geoid					Quasigeoid				
(Mean distance)	min (m)	max (m)	mean (m)	STD (m)	Average ppm	min (m)	max (m)	mean (m)	STD (m)	Average ppm
India (713.46 km)	-0.620	1.684	0.373	±0.418	3.371	-0.625	1.632	0.368	±0.408	3.362
UP west (197.28 km)	-0.605	0.743	0.040	±0.191	1.111	-0.602	0.742	0.057	±0.193	1.118
UP east (169.33 km)	-0.374	0.367	0.015	±0.161	1.048	-0.372	0.367	0.018	±0.161	1.052
Hyderabad (18.67 km)	-0.620	0.886	-0.031	±0.221	13.032	-0.625	0.888	-0.032	±0.221	13.025
Bangalore (14.08 km)	-0.074	0.079	-0.005	±0.044	3.113	-0.077	0.081	-0.008	±0.046	3.281

648

649

650 Table 3: Comparison of EIGEN-6C4 and IndGG-CUT2021 validated with GNSS/levelling data (Units in m).

		min	max	mean	STD
India	**EIGEN-6C4**	-1.203	0.463	-0.428	±0.410
	IndGG-CUT2021	-0.897	0.788	-0.171	±0.396
UP west	**EIGEN-6C4**	-1.203	-0.643	-0.870	±0.105
	IndGG-CUT2021	-0.897	-0.154	-0.532	±0.138
UP east	**EIGEN-6C4**	-1.034	-0.361	-0.742	±0.144
	IndGG-CUT2021	-0.712	-0.338	-0.521	±0.114
Hyderabad	**EIGEN-6C4**	-0.612	0.258	-0.154	±0.157
	IndGG-CUT2021	-0.385	0.501	0.070	±0.158
Bangalore	**EIGEN-6C4**	0.379	0.463	0.422	±0.029
	IndGG-CUT2021	0.709	0.788	0.751	±0.030

651